

Published in final edited form as:

DNA Repair (Amst). 2013 September ; 12(9): 707–712. doi:10.1016/j.dnarep.2013.05.004.

Functional Attributes of the *S. cerevisiae* Meiotic Recombinase Dmc1

Valeria Busygina^{a,*}, William A. Gaines^{a,*}, Yuanyuan Xu^a, Youngho Kwon^a, Gareth J. Williams^b, Sheng-Wei Lin^c, Hao-Yen Chang^d, Peter Chi^{c,d}, Hong-Wei Wang^e, and Patrick Sung^{a,†}

^aDepartment of Molecular Biophysics and Biochemistry, Yale University School of Medicine, New Haven, Connecticut 06520, USA

^bLife Science Division, Lawrence Berkeley National Laboratory, Berkeley, California 94720, USA

^cInstitute of Biological Chemistry, Academia Sinica, 128 Academia Road, Section 2, Nankang, Taipei 115, Taiwan

^dInstitute of Biochemical Sciences, National Taiwan University, No. 1, Section 4, Roosevelt Road, Taipei, 10617, Taiwan

^eTsinghua-Peking Center for Life Sciences, Center for Structural Biology, School of Life Sciences, Tsinghua University, Beijing 100084, China

Abstract

The role of Dmc1 as a meiosis-specific general recombinase was first demonstrated in *S. cerevisiae*. Progress in understanding the biochemical mechanism of ScDmc1 has been hampered by its tendency to form inactive aggregates. We have found that the inclusion of ATP during protein purification prevents Dmc1 aggregation. ScDmc1 so prepared is capable of forming D-loops and responsive to its accessory factors Rad54 and Rdh54. Negative staining electron microscopy and iterative helical real-space reconstruction revealed that the ScDmc1-ssDNA nucleoprotein filament harbors 6.5 protomers per turn with a pitch of ~106 Å. The ScDmc1 purification procedure and companion molecular analyses should facilitate future studies on this recombinase.

Keywords

Dmc1 recombinase; homologous recombination; meiosis

© 2013 Elsevier B.V. All rights reserved.

[†]To whom correspondence should be addressed: Department of Molecular Biophysics and Biochemistry, Yale University School of Medicine, 333 Cedar St., SHM-C130, New Haven, CT 06520-8024, United States. Tel.: 203-785-4569; Fax: 203-785-6404; Patrick.Sung@yale.edu.

*These authors contributed equally to this work.

Conflict of interest statement: The authors declare that there are no conflicts of interest.

Publisher's Disclaimer: This is a PDF file of an unedited manuscript that has been accepted for publication. As a service to our customers we are providing this early version of the manuscript. The manuscript will undergo copyediting, typesetting, and review of the resulting proof before it is published in its final citable form. Please note that during the production process errors may be discovered which could affect the content, and all legal disclaimers that apply to the journal pertain.

1. Introduction

During meiosis I, homologous chromosomes become aligned and separated into different cells, thus halving the chromosome number. Chromosome disjunction in meiosis I is dependent upon the formation of physical connections between chromosome pairs through homologous recombination (HR) that is triggered by DNA double-strand breaks (DSBs) introduced by the Spo11 complex [1].

In the HR reaction, the DSB ends undergo 5' strand resection to generate 3' ssDNA tails that are bound by either of the two conserved recombinases, Dmc1 and Rad51. Polymerization of these recombinases onto the ssDNA tails yields a helical nucleoprotein filament, termed the presynaptic filament, that is capable of catalyzing the formation of a DNA strand invasion product, called the D-loop, with a homologous chromatid. Unlike Dmc1, which is strictly meiosis-specific, Rad51 functions in both meiotic and mitotic cells [2,3].

Meiotic HR is marked by a high level of interhomolog crossovers, which tie the homologous chromosome pairs to ensure their orderly segregation in meiosis I [1,4]. Accordingly, mutations in either *RAD51* or *DMC1* result in chromosome non-disjunction in meiosis. However, Dmc1 is more adept at generating interhomolog crossovers than Rad51. As such, Dmc1 helps establish the proper inter-homolog bias of meiotic DSB repair [5,6]. Interestingly, recent evidence implicates Rad51 as a Dmc1 cofactor. In this regard, Rad51 must bind ssDNA, but its recombinase activity is dispensable [7].

Here, we describe a ScDmc1 purification method that yields unaggregated, biochemically active recombinase. We clarify the relationship of Dmc1 with two known accessory factors, Rad54 and Rdh54. In addition, we provide a 3D reconstruction of the ScDmc1 presynaptic filament based on electron microscopic analyses. The reconstruction has revealed structural features of the ScDmc1 presynaptic filament in common with those made by other general recombinases.

2. Materials and Methods

2.1. Expression and Purification of ScDmc1

The pNRB150 vector harboring N-terminally (His)₆-tagged ScDmc1 [8] was introduced into BL21[DE3] Rosetta cells (Novagen). The (His)₆ tagged ScDmc1 has been previously demonstrated to retain biological function *in vivo* [8], even though a slight perturbation in protein properties by the tag remains possible. An overnight bacterial culture was diluted 50 fold in 2xLB media supplemented with ampicillin (100 µg/ml) and chloramphenicol (34 µg/ml) and grown at 37°C to OD₆₀₀ = 0.8. ScDmc1 expression was induced with 0.1 mM IPTG for 16 hours at 16°C. Cell lysate preparation and all the protein purification steps were conducted at 4°C in buffer T (25 mM Tris-HCl, pH 7.4, 10% glycerol, 0.5 mM EDTA, 0.01% IGEPAL CA-630 (Sigma), 1 mM DTT) supplemented with 2 mM ATP and 2 mM MgCl₂. We note that 0.1 mM Na₃VO₄ was routinely included in these buffers to preserve the ATP concentration as it inhibits various enzymes that hydrolyze ATP, but its omission does not affect the oligomeric state or biochemical activities of Dmc1 (data not shown). Chromatographic column fractions were screened for their ScDmc1 content by 12% SDS-PAGE and Coomassie Blue staining. We prepared lysate from 20 g of *E. coli* paste in 100 ml of buffer supplemented with 500 mM KCl, 1 mM phenylmethylsulfonyl fluoride, 0.5 mM benzamidine and 5 µg/ml each of aprotinin, chymostatin, leupeptin, and pepstatin. Cells were disrupted by sonication. After ultracentrifugation (100,000 × g for 90 min), the lysate was incubated with 2 ml of Talon affinity resin (Clontech) for 2 hours with gentle mixing. The matrix was poured into a column with an internal diameter of 1 cm and washed

sequentially with 20 ml of buffer with 500 mM KCl and with 150 mM KCl, respectively, followed by ScDmc1 elution using buffer supplemented with 150 mM KCl and 200 mM imidazole. The protein pool was diluted with an equal volume of buffer T and fractionated in a 1 ml Heparin Sepharose column (GE Healthcare) with a 30 ml gradient of 150–1000 mM KCl, collecting 1 ml fractions. Fractions containing ScDmc1 (eluting at ~500 mM KCl) were pooled, diluted to the conductivity of 150 mM KCl and further fractionated in a 1 ml Mono Q column with a 30 ml gradient of 150–500 mM KCl, collecting 1 ml fractions. Fractions containing ScDmc1 (eluting at ~300 mM KCl) were pooled, concentrated in an Amicon Ultra micro-concentrator (Millipore), snap-frozen in liquid nitrogen, and stored at -80°C . The yield of highly purified ScDmc1 was 7 to 10 mg.

2.2. Other proteins

hDMC1, Rad54 and Rdh54 were expressed and purified as described previously [9–11]. To aid in purification, hDMC1 was tagged with (His)₆ at its N-terminus while Rad54 and Rdh54 were both tagged with a compound thioredoxin-(His)₆-S tag at their N-terminus [10,11].

2.3. Gel filtration analysis

ScDmc1 prepared without or with ATP-Mg²⁺ was analyzed in a Superdex 200 PC 3.2/30 size exclusion column (GE Healthcare) equilibrated in buffer T with 300 mM KCl and 2 mM each of ATP and Mg²⁺. Fractions were analyzed by SDS-PAGE with silver staining. Purified hDMC1 was similarly analyzed.

2.4. DNA binding assay

ScDmc1 (0.09, 0.18, 0.27, 0.36 and 0.45 μM) was incubated with radiolabeled 83-mer ssDNA (2.7 μM nucleotides) or dsDNA (2.7 μM base pairs) [12] in buffer A (35 mM Tris, pH 7.5, 1 mM DTT, 100 ng/ μl BSA, 1.5 mM CaCl₂, 1.5 mM MgCl₂, 4 mM ATP, and 100 mM KCl) for 3 min at 37°C. DNA species were resolved by electrophoresis in a 10% polyacrylamide gel run in TB buffer (90 mM Tris, 90 mM boric acid, pH 8.3) and analyzed by phosphorimaging.

2.5. ATPase assay

ScDmc1 (3.2 μM) was incubated in buffer D (50 mM Tris, pH 7.5, 1 mM DTT) containing 125 μM ATP, 0.02 μCi [α -³²P] ATP, 100 mM KCl, 1.5 mM MgCl₂, and with or without 1.5 mM CaCl₂ in the presence of pBluescript ssDNA (45 μM nucleotides) or linear dsDNA (45 μM base pairs) at 37°C. At the indicated times (3, 5, 10, and 15 minutes), a 1 μl aliquot was taken and mixed with an equal volume of 500 mM EDTA to halt ATP hydrolysis. The level of ATP hydrolysis was determined by thin-layer chromatography and phosphorimaging analysis [13].

2.6. D-loop assay

The D-loop reaction was conducted as described [8,10]. Briefly, ScDmc1 was incubated with the ³²P-labeled 90-mer oligonucleotide substrate (3 μM nucleotides) at 37°C for 5 min. Next, Rad54 or Rdh54 was added. The reaction was initiated by the addition of pBluescript SK replicative form I DNA (72 μM base pairs). The reaction (25 μl final volume) had a buffer composition of 50 mM Tris-HCl, pH 7.5, 1 mM DTT, 72 mM KCl, 1 mM MgCl₂, 5 mM CaCl₂, and 4 mM ATP with an ATP regenerating system (20 mM creatine phosphate, 30 $\mu\text{g/ml}$ creatine kinase). After a 15-min incubation at 30°C, SDS (1%) and proteinase K (1 mg/ml) were added, followed by a 5-min incubation at 37°C. The deproteinized samples were subject to electrophoresis in a 0.9% agarose gel and analyzed by phosphorimaging. In Figure 3, 1.0, 1.6, and 2 μM of ScDmc1 were used. In Figure 4, 1.6 μM of ScDmc1 and

150, 300 or 500 nM of Rad54 or Rdh54 were used. In Figure S2 1.6 μM of ScDmc1 and 300 or 500 nM of Rad54 or Rdh54 were used.

2.7. Homologous DNA strand exchange assay

The oligonucleotide-based DNA strand exchange assay was carried out as described [14]. Briefly, ScDmc1 (1.6, 2.0, 2.5, 3.2, and 4 μM) was incubated with 150-mer ssDNA oligonucleotide (6 μM nucleotides) in 10.5 μl of buffer D containing 30 mM KCl, 2 mM ATP, 2 mM CaCl_2 , and 5 mM MgCl_2 for 5 min at 37°C. Then, 1 μl of 50 mM spermidine and 1 μl of ^{32}P -labeled homologous 40-mer dsDNA (6 μM base pairs) were added to complete the reaction. Following incubation at 37°C for 30 min, the reaction was deproteinized and subject to electrophoresis in a 10% polyacrylamide gel run in TAE buffer (40mM Tris acetate, pH 7.4, 0.5mM EDTA). Analysis was by phosphorimaging.

2.8. Affinity pulldown assay

ScDmc1 (5 μg) was incubated with S-tagged Rad54 or Rdh54 (10 μg) in 30 μl of buffer B (20 mM K_2HPO_4 , pH 7.5, 10% glycerol, 150 mM KCl, 0.01% IGEPAL, 1 mM DTT) for 30 min at 4°C. The reaction mixtures were mixed with 10 μl of S-protein agarose (Novagen) and incubated for 30 min at 4°C with gentle agitation. The resin was washed twice with 200 μl of buffer B and bound proteins were eluted with 20 μl 2% SDS. The Supernatant (S), elution (E), and wash (W) fractions, 10 μl each, were analyzed by 12% SDS-PAGE followed by Coomassie Blue staining or western blot with anti-hDMC1 antibody (Santa Cruz Biotechnology, catalogue #22768), which is reactive toward ScDmc1.

2.9. Electron microscopy and 3D reconstructions

To prepare presynaptic filaments, human or *S. cerevisiae* Dmc1 (2 μM each) was incubated with a 150-mer ssDNA oligonucleotide (6 μM nucleotides) in buffer E (25 mM HEPES, pH 7.5, 1 mM DTT) containing 100 mM KCl (for hDMC1 only) and either 2 mM MgCl_2 with 2 mM AMP-PNP or 2 mM CaCl_2 with 2 mM ATP for 5 min (ScDmc1) or 20 min (hDMC1) at 37°C. The filaments were applied onto carbon-coated grids that were freshly glow-discharged in a plasma cleaner apparatus and stained with 2% (w/v) uranyl formate. The grids were examined in an FEI Tecnai 12 electron microscope operated at 120 kV with a nominal magnification of 42,000. Images were recorded on a Gatan Ultrascan4000 4kx4k CCD camera with a pixel size of 5.6 Å. The defocus used was about 0.7 μm . Segments of hDMC1-ssDNA-AMP-PNP, ScDmc1-ssDNA-AMP-PNP and ScDmc1-ssDNA-ATP were extracted into 50x50-pixel boxes with 90% overlapping using the BOXER program of EMAN [15]. The segments were processed using custom scripts in the SPIDER package [16]. The IHRSR package was used for the final helical reconstruction [17,18]. Model docking and demonstration were performed in UCSF-Chimera [19]. Datasets of hDMC1-ssDNA-AMP-PNP (n = 10,467 segments), ScDmc1-ssDNA-AMP-PNP (n = 9,879 segments) and ScDmc1-ssDNA-ATP filaments (n = 11,254 segments) were pooled for the 3D reconstructions.

3. Results

3.1. Prevention of ScDmc1 aggregation via ATP inclusion

Even though we can readily obtain human and *S. pombe* Dmc1 proteins in an unaggregated form [9,20–23], our attempts to isolate biochemically active *S. cerevisiae* Dmc1 (ScDmc1) have been hampered by its aggregation during purification [7,24]. Since Dmc1 must bind ATP when functioning as a recombinase, we tested if the inclusion of ATP during cell extract preparation and in chromatographic column buffers would prevent protein aggregation (Figure 1A). When analyzed by gel filtration in a Superdex 200 column, ScDmc1 purified without ATP appeared near the void volume (>1 MDa) with significant

trailing, whereas protein preparations obtained with ATP present appeared as a broad peak spanning from 260 kDa to 510 kDa with some trailing into the lower molecular weight range (Figure 1B). This broad peak is similar to what has been observed for human RAD51 when analyzed by gel filtration [25]. We note that human DMC1 (hDMC1), being octameric [26], eluted within a similar size range as ScDmc1 when subject to the same analysis. Thus, ATP appears to prevent aggregation of ScDmc1, and the biochemical analyses presented below provide evidence that the inclusion of ATP during ScDmc1 purification preserves its biological activity. For the remainder of this report, the ScDmc1 preparations obtained with ATP present will be referred to as ScDmc1, whereas the preparations made without ATP as “aggregated ScDmc1”.

3.2. Ca^{2+} attenuates ATP hydrolysis by ScDmc1 and stabilizes ScDmc1 association with DNA

Rad51 and Dmc1 from different organisms have been shown to hydrolyze ATP with a dependence on DNA. Moreover, there is substantial evidence that ATP hydrolysis prompts the turnover of recombinase molecules from bound DNA [27,28]. We found that our ScDmc1 preparations also possess an ATPase activity that is stimulated strongly by DNA, with ssDNA being the more efficacious cofactor (Figures 2A and 2B). Even though ScDmc1 clearly has a DNA-dependent ATPase activity, a nucleoprotein complex of it with DNA in the presence of ATP and Mg^{2+} could only be observed at a very low KCl concentration of 20 mM (data not shown), suggesting either a low affinity of ScDmc1 for DNA and/or an inherent instability of the nucleoprotein complexes that form.

Ca^{2+} has been shown to attenuate ATP hydrolysis by human RAD51 and DMC1 proteins, leading to stabilization of the presynaptic filament [29]. Consistent with this, we discovered that, upon the inclusion of Ca^{2+} in the reaction buffer, ScDmc1 associates with ssDNA and dsDNA stably to cause a mobility shift of the DNA in gel electrophoresis (Figure 2C). In this regard, ScDmc1 appears to have a higher affinity for ssDNA (Figure 2C, panel iii). We note that the aggregated ScDmc1 is devoid of DNA binding activity under the same reactions used above (data not shown). As expected, the rate of DNA-dependent ATP hydrolysis by ScDmc1 is reduced when Ca^{2+} is present (Figure 2B).

3.3. Regulation of Dmc1-mediated homologous DNA pairing by Ca^{2+} ions

We examined ScDmc1 for the ability to form D-loops, by carrying out the reaction using ATP as a cofactor and with Mg^{2+} only or with Ca^{2+} also present. The results showed clearly that D-loop formation is contingent upon the addition of Ca^{2+} (Figure 3B). By using linear ssDNA and dsDNA as substrates, we further verified that the ability of ScDmc1 to make DNA joints is greatly enhanced by Ca^{2+} (Supplementary figure S1). Importantly, in the presence of AMP-PNP, D-loop formation was seen even with Mg^{2+} alone (Figure 3B). These results provide support for the premise that ScDmc1 fails to form a stable enough presynaptic filament capable of homologous DNA pairing unless ATP hydrolysis is attenuated (via the inclusion of Ca^{2+}) or when the non-hydrolyzable analog AMP-PNP is used. In contrast, the aggregated ScDmc1 showed little or no homologous DNA pairing activity under all the conditions tested (data not shown).

3.4. Enhancement of Dmc1-mediated homologous pairing by Rad54 and Rdh54

Rad54 and Rdh54, members of the Swi2/Snf2 family of DNA translocases, participate in HR in vegetative and meiotic cells. There is substantial evidence that these DNA motor proteins and their orthologs enhance the activity of Rad51 and Dmc1 in the HR reaction [9,23,24,30,31]. By affinity pulldown, we verified that ScDmc1 interacts physically with Rad54 and Rdh54 (Figure 4A). Importantly, our results also showed that, in the presence of Ca^{2+} , Rad54 and Rdh54 greatly enhance the ability of Dmc1 to form D-loops (Figure 4B).

As we had anticipated, the aggregated Dmc1 is unable to form a significant amount of D-loop even when Rad54 or Rdh54 is present (Supplementary figure S2). We note, however, that the aggregated protein is still able to physically interact with Rad54 and Rdh54 (Supplementary figure S3).

3.5. Three-dimensional reconstruction of the ScDmc1 presynaptic filament

We endeavored to determine the 3D structure of the ScDmc1 presynaptic filament. To do this, ScDmc1 was incubated with a 150-mer ssDNA oligonucleotide with AMP-PNP-Mg²⁺ as cofactor and then the presynaptic filament was subject to negative staining electron microscopy coupled with iterative helical real-space reconstruction (IHRSR) [17,18]. Like equivalent presynaptic filaments made with hDMC1, the ScDmc1 presynaptic filaments exhibited a strong helical pattern (Figure 5). The same helical pattern was observed with ScDmc1 filaments formed with ATP-Ca²⁺ except the filament length was longer in general (Figure 5), which could stem from end-to-end stacking of individual filaments [32]. Consistent with previous studies [26,33], hDMC1 formed stacked rings on DNA upon omission of ATP (data not shown). In contrast, ScDmc1 formed only irregularly-shaped aggregates when ATP was absent (data not shown), further illustrating the importance of ATP in the maintenance of protein activity. 3D reconstructions revealed that both the ScDmc1 and hDMC1 filaments possess a right-handedness, 6.5 protomers per turn, with a helical pitch of ~106 Å. The hDMC1 presynaptic filaments exhibited nearly full density expected for the N-terminal domain (NTD) (Figure 5B, arrow). In contrast, the 3D reconstruction of ScDmc1 presynaptic filaments showed less density for the NTD (Figure 5A, arrows), suggesting a higher degree of flexibility of this domain in the yeast protein.

4. Discussion

Even though biochemically active preparations of (His)₆-tagged and GST-tagged ScDmc1 have been described by two other groups [8,24], in our hands, the (His)₆-tagged recombinase [8] undergoes rapid aggregation unless ATP is included in the buffers used in protein purification. Making use of our newly developed purification protocol, ScDmc1 can be obtained with a high yield and consistent biochemical activities, including the formation of right-handed helical filaments on ssDNA, DNA-dependent ATPase, DNA binding, and homologous DNA pairing and strand exchange activities. Moreover, we have provided evidence for physical and functional interactions of ScDmc1 with both Rad54 and Rdh54. These results are in general congruence with published data on Dmc1 homologs from multiple organisms [9,11,24,29,34].

Several functional aspects of ScDmc1 are worth highlighting. First, the ScDmc1 protein filament on either ssDNA or dsDNA is surprisingly unstable unless ATP hydrolysis is attenuated via the inclusion of Ca²⁺ in the reaction buffer. Likewise, ScDmc1 is unable to promote homologous DNA pairing with ATP as cofactor unless Ca²⁺ is also added ([24,29]; this work). Alternatively, assembly of a stable ScDmc1 presynaptic filament capable of homologous DNA pairing can be achieved using the non-hydrolyzable ATP analog AMP-PNP ([29]; this work). Since the intracellular concentration of free Ca²⁺ is quite low [35], it seems likely that ScDmc1 accessory factors, e.g. the conserved Hop2-Mnd1 and Mei5-Sae3 complexes [22,36–38], may fulfill the ScDmc1 presynaptic filament stabilization role in meiosis. In addition, ScRad51, as an accessory factor for ScDmc1 [7], may also contribute toward the assembly and/or maintenance of the ScDmc1 presynaptic filament.

Aside from the biochemical analyses, we have presented herein the 3D reconstruction of the ScDmc1 presynaptic filament based on negative stain electron microscopy. A study comparing the structures of ScRad51, hRAD51, and hDMC1 presynaptic filaments indicated that they share structural similarities [39]. Our 3D reconstruction of the ScDmc1 presynaptic

filament has now revealed common structural features with presynaptic filaments of these other recombinases. Specifically, like the other recombinase presynaptic filaments, the ScDmc1 presynaptic filament has right-handedness, harbors 6.5 protomers per turn, and possesses a helical pitch of ~ 106 Å. We note that there has been a disagreement on the helical symmetry of the hDMC1 presynaptic filament, with one study reporting 9 units/helical turn [40] and another supporting 6.5 units/helical turn [41]. Our 3D reconstructions here of both hDMC1 and ScDmc1 presynaptic filaments support the 6.5 units/turn helical parameter [39].

In conclusion, the ScDmc1 purification protocol we have developed will likely be valuable for the ongoing mechanistic dissection of the role of Dmc1 in meiotic recombination in *S. cerevisiae*, in particular for examining its recombinase activity, alone and in combination with various accessory factors, such as those mentioned above.

Supplementary Material

Refer to Web version on PubMed Central for supplementary material.

Acknowledgments

We are grateful to Douglas Bishop for the (His)₆-ScDmc1 expression plasmid and to Edward Egelman for the IHRSR processing package used in the 3D reconstructions. Image acquisition and processing were conducted in the Yale CryoEM and High Performance Computational facilities. This study was supported by NIH grants RO1GM057814, RO1ES007061, and PO1CA092584, NIH postdoctoral fellowship F32GM101808, National Science Council of Taiwan grant NSC 100-2311-B-002-009, National Taiwan University grants 102R7848 and 102R7560-6, National Basic Research Program of China grant 2010CB912401, and the National Center for Protein Sciences Beijing.

Abbreviations

HR	homologous recombination
DSB	double-strand break
NTD	N-terminal domain

References

1. Neale MJ, Keeney S. Clarifying the mechanics of DNA strand exchange in meiotic recombination. *Nature*. 2006; 442:153–158. [PubMed: 16838012]
2. Bishop DK, Park D, Xu L, Kleckner N. DMC1: a meiosis-specific yeast homolog of *E. coli* recA required for recombination, synaptonemal complex formation, and cell cycle progression. *Cell*. 1992; 69:439–456. [PubMed: 1581960]
3. Shinohara A, Shinohara M. Roles of RecA homologues Rad51 and Dmc1 during meiotic recombination. *Cytogenetic and genome research*. 2004; 107:201–207. [PubMed: 15467365]
4. Bishop DK, Zickler D. Early decision; meiotic crossover interference prior to stable strand exchange and synapsis. *Cell*. 2004; 117:9–15. [PubMed: 15066278]
5. Tsubouchi H, Roeder GS. The importance of genetic recombination for fidelity of chromosome pairing in meiosis. *Developmental cell*. 2003; 5:915–925. [PubMed: 14667413]
6. Sheridan S, Bishop DK. Red-Hed regulation: recombinase Rad51, though capable of playing the leading role, may be relegated to supporting Dmc1 in budding yeast meiosis. *Genes & development*. 2006; 20:1685–1691. [PubMed: 16818601]
7. Cloud V, Chan YL, Grubb J, Budke B, Bishop DK. Rad51 is an accessory factor for Dmc1-mediated joint molecule formation during meiosis. *Science (New York, NY)*. 2012; 337:1222–1225.

8. Hong EL, Shinohara A, Bishop DK. *Saccharomyces cerevisiae* Dmc1 protein promotes renaturation of single-strand DNA (ssDNA) and assimilation of ssDNA into homologous super-coiled duplex DNA. *The Journal of biological chemistry*. 2001; 276:41906–41912. [PubMed: 11551925]
9. Sehorn MG, Sigurdsson S, Bussen W, Unger VM, Sung P. Human meiotic recombinase Dmc1 promotes ATP-dependent homologous DNA strand exchange. *Nature*. 2004; 429:433–437. [PubMed: 15164066]
10. Raschle M, Van Komen S, Chi P, Ellenberger T, Sung P. Multiple interactions with the Rad51 recombinase govern the homologous recombination function of Rad54. *The Journal of biological chemistry*. 2004; 279:51973–51980. [PubMed: 15465810]
11. Chi P, Kwon Y, Seong C, Epshtein A, Lam I, Sung P, Klein HL. Yeast recombination factor Rdh54 functionally interacts with the Rad51 recombinase and catalyzes Rad51 removal from DNA. *The Journal of biological chemistry*. 2006; 281:26268–26279. [PubMed: 16831867]
12. Krejci L, Song B, Bussen W, Rothstein R, Mortensen UH, Sung P. Interaction with Rad51 is indispensable for recombination mediator function of Rad52. *The Journal of biological chemistry*. 2002; 277:40132–40141. [PubMed: 12171935]
13. Petukhova G, Stratton S, Sung P. Catalysis of homologous DNA pairing by yeast Rad51 and Rad54 proteins. *Nature*. 1998; 393:91–94. [PubMed: 9590697]
14. San Filippo J, Chi P, Sehorn MG, Etchin J, Krejci L, Sung P. Recombination mediator and Rad51 targeting activities of a human BRCA2 polypeptide. *The Journal of biological chemistry*. 2006; 281:11649–11657. [PubMed: 16513631]
15. Ludtke SJ, Baldwin PR, Chiu W. EMAN: semiautomated software for high-resolution single-particle reconstructions. *Journal of structural biology*. 1999; 128:82–97. [PubMed: 10600563]
16. Frank J, Radermacher M, Penczek P, Zhu J, Li Y, Ladjadj M, Leith A. SPIDER and WEB: processing and visualization of images in 3D electron microscopy and related fields. *Journal of structural biology*. 1996; 116:190–199. [PubMed: 8742743]
17. Egelman EH. A robust algorithm for the reconstruction of helical filaments using single-particle methods. *Ultramicroscopy*. 2000; 85:225–234. [PubMed: 11125866]
18. Egelman EH. The iterative helical real space reconstruction method: surmounting the problems posed by real polymers. *Journal of structural biology*. 2007; 157:83–94. [PubMed: 16919474]
19. Goddard TD, Huang CC, Ferrin TE. Visualizing density maps with UCSF Chimera. *Journal of structural biology*. 2007; 157:281–287. [PubMed: 16963278]
20. Gupta RC, Golub E, Bi B, Radding CM. The synaptic activity of HsDmc1, a human recombination protein specific to meiosis. *Proceedings of the National Academy of Sciences of the United States of America*. 2001; 98:8433–8439. [PubMed: 11459986]
21. Sauvageau S, Stasiak AZ, Banville I, Ploquin M, Stasiak A, Masson JY. Fission yeast rad51 and dmc1, two efficient DNA recombinases forming helical nucleoprotein filaments. *Molecular and cellular biology*. 2005; 25:4377–4387. [PubMed: 15899844]
22. Haruta N, Kurokawa Y, Murayama Y, Akamatsu Y, Unzai S, Tsutsui Y, Iwasaki H. The Swi5-Sfr1 complex stimulates Rhp51/Rad51- and Dmc1-mediated DNA strand exchange in vitro. *Nature structural & molecular biology*. 2006; 13:823–830.
23. Chi P, Kwon Y, Moses DN, Seong C, Sehorn MG, Singh AK, Tsubouchi H, Greene EC, Klein HL, Sung P. Functional interactions of meiotic recombination factors Rdh54 and Dmc1. *DNA repair*. 2009; 8:279–284. [PubMed: 19028606]
24. Nimonkar AV, Dombrowski CC, Siino JS, Stasiak AZ, Stasiak A, Kowalczykowski SC. *Saccharomyces cerevisiae* Dmc1 and Rad51 proteins preferentially function with Tid1 and Rad54 proteins, respectively, to promote DNA strand invasion during genetic recombination. *The Journal of biological chemistry*. 2012; 287:28727–28737. [PubMed: 22761450]
25. Esashi F, Galkin VE, Yu X, Egelman EH, West SC. Stabilization of RAD51 nucleoprotein filaments by the C-terminal region of BRCA2. *Nature structural & molecular biology*. 2007; 14:468–474.
26. Passy SI, Yu X, Li Z, Radding CM, Masson JY, West SC, Egelman EH. Human Dmc1 protein binds DNA as an octameric ring. *Proceedings of the National Academy of Sciences of the United States of America*. 1999; 96:10684–10688. [PubMed: 10485886]

27. Chi P, Van Komen S, Sehorn MG, Sigurdsson S, Sung P. Roles of ATP binding and ATP hydrolysis in human Rad51 recombinase function. *DNA repair*. 2006; 5:381–391. [PubMed: 16388992]
28. Chen Z, Yang H, Pavletich NP. Mechanism of homologous recombination from the RecA-ssDNA/dsDNA structures. *Nature*. 2008; 453:489–484. [PubMed: 18497818]
29. Lee MH, Chang YC, Hong EL, Grubb J, Chang CS, Bishop DK, Wang TF. Calcium ion promotes yeast Dmc1 activity via formation of long and fine helical filaments with single-stranded DNA. *The Journal of biological chemistry*. 2005; 280:40980–40984. [PubMed: 16204247]
30. Klein HL. RDH54, a RAD54 homologue in *Saccharomyces cerevisiae*, is required for mitotic diploid-specific recombination and repair and for meiosis. *Genetics*. 1997; 147:1533–1543. [PubMed: 9409819]
31. Shinohara M, Shita-Yamaguchi E, Buerstedde JM, Shinagawa H, Ogawa H, Shinohara A. Characterization of the roles of the *Saccharomyces cerevisiae* RAD54 gene and a homologue of RAD54, RDH54/TID1, in mitosis and meiosis. *Genetics*. 1997; 147:1545–1556. [PubMed: 9409820]
32. Galkin VE, Yu X, Bielnicki J, Ndjonka D, Bell CE, Egelman EH. Cleavage of bacteriophage lambda cI repressor involves the RecA C-terminal domain. *Journal of molecular biology*. 2009; 385:779–787. [PubMed: 19013467]
33. Masson JY, Davies AA, Hajibagheri N, Van Dyck E, Benson FE, Stasiak AZ, Stasiak A, West SC. The meiosis-specific recombinase hDmc1 forms ring structures and interacts with hRad51. *The EMBO journal*. 1999; 18:6552–6560. [PubMed: 10562567]
34. Bugreev DV, Golub EI, Stasiak AZ, Stasiak A, Mazin AV. Activation of human meiosis-specific recombinase Dmc1 by Ca²⁺. *The Journal of biological chemistry*. 2005; 280:26886–26895. [PubMed: 15917244]
35. Cunningham KW, Fink GR. Ca²⁺ transport in *Saccharomyces cerevisiae*. *The Journal of experimental biology*. 1994; 196:157–166. [PubMed: 7823019]
36. Tsubouchi H, Roeder GS. The budding yeast mei5 and sae3 proteins act together with dmc1 during meiotic recombination. *Genetics*. 2004; 168:1219–1230. [PubMed: 15579681]
37. Chi P, San Filippo J, Sehorn MG, Petukhova GV, Sung P. Bipartite stimulatory action of the Hop2-Mnd1 complex on the Rad51 recombinase. *Genes & development*. 2007; 21:1747–1757. [PubMed: 17639080]
38. Pezza RJ, Voloshin ON, Vanevski F, Camerini-Otero RD. Hop2/Mnd1 acts on two critical steps in Dmc1-promoted homologous pairing. *Genes & development*. 2007; 21:1758–1766. [PubMed: 17639081]
39. Sheridan SD, Yu X, Roth R, Heuser JE, Sehorn MG, Sung P, Egelman EH, Bishop DK. A comparative analysis of Dmc1 and Rad51 nucleoprotein filaments. *Nucleic acids research*. 2008; 36:4057–4066. [PubMed: 18535008]
40. Okorokov AL, Chaban YL, Bugreev DV, Hodgkinson J, Mazin AV, Orlova EV. Structure of the hDmc1-ssDNA filament reveals the principles of its architecture. *PloS one*. 2010; 5:e8586. [PubMed: 20062530]
41. Yu X, Egelman EH. Helical filaments of human Dmc1 protein on single-stranded DNA: a cautionary tale. *Journal of molecular biology*. 2010; 401:544–551. [PubMed: 20600108]

Highlights

- Inclusion of ATP and Mg²⁺ during purification prevents ScDmc1 aggregation.
- ScDmc1 so purified is active as recombinase and responsive to Rad54 and Rdh54.
- 3D reconstruction of ScDmc1 on ssDNA illustrates likeness with other recombinases.

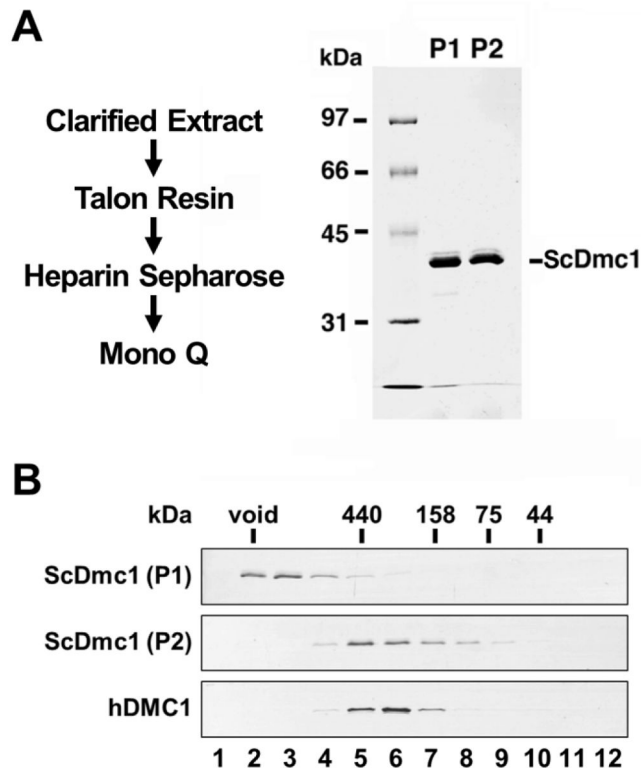


Figure 1. ScDmc1 purification

A. Schematic of purification procedure and SDS-PAGE of ScDmc1 (1 μ g of protein in each lane) purified without ATP (P1) or with ATP present (P2). **B.** Analysis of ScDmc1 purified without or with ATP and of hDMC1 in a column of Superdex 200 gel filtration resin. The void volume was determined by elution of Dextran Blue and the elution positions of the size standards are indicated: Ferritin (440 kDa), Aldolase (158 kDa), Conalbumin (75 kDa), and Ovalbumin (44 kDa).

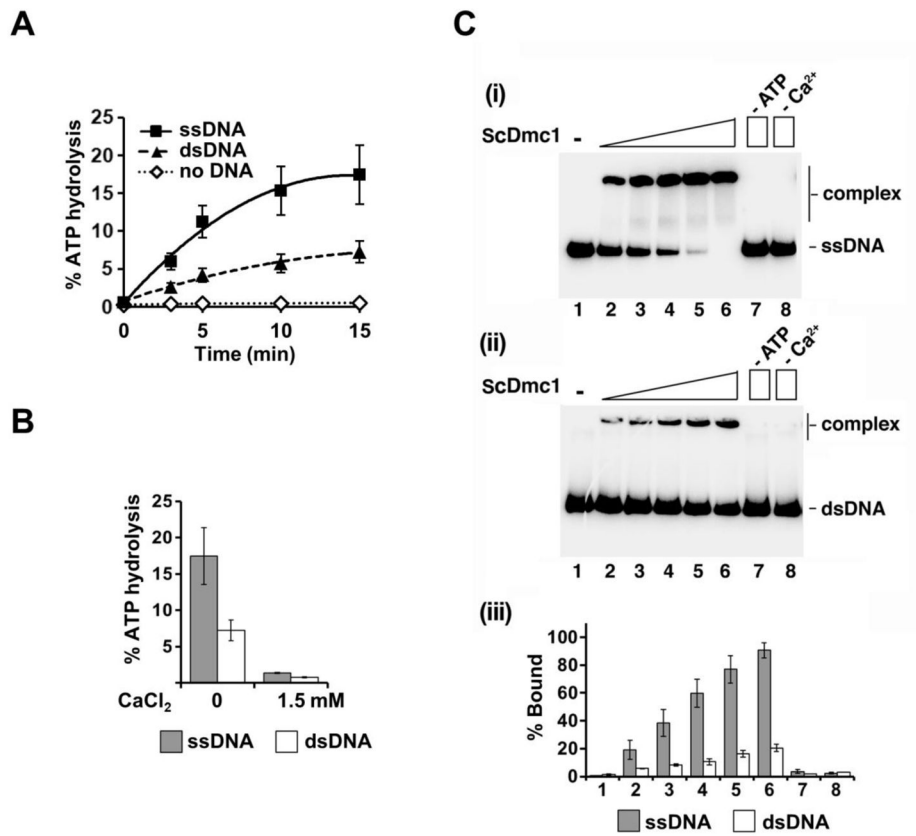


Figure 2. Effect of Ca²⁺ on ATP hydrolysis and DNA binding by ScDmc1
A. ATP hydrolysis by ScDmc1 was examined without or with ssDNA or dsDNA, and the results were graphed (n=3, +/- standard error). **B.** DNA-dependent ATP hydrolysis by ScDmc1 was examined with and without CaCl₂, and the results were graphed (n=3, +/- standard error). The incubation time was 15 min. **C.** Binding of ³²P labeled 83-mer ssDNA **(i)** or dsDNA **(ii)** by ScDmc1 was examined. The results were graphed **(iii)** (n=3, +/- standard error).

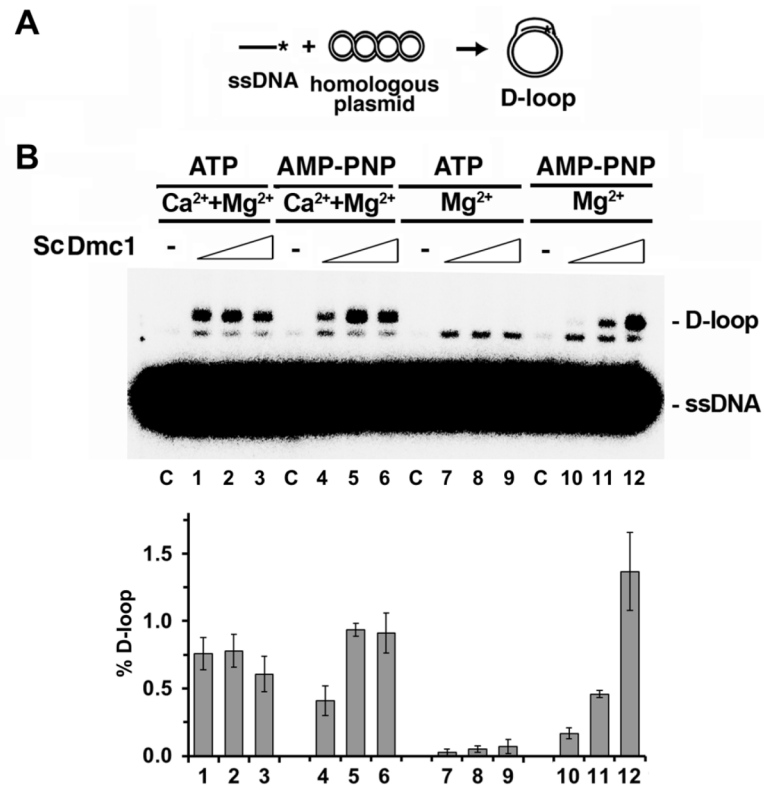


Figure 3. Effects of Ca²⁺ and AMP-PNP on the homologous DNA pairing activity of ScDmc1
A. Schematic of the D-loop reaction. **B.** D-loop formation by ScDmc1 was examined in the presence of Ca²⁺, Mg²⁺, ATP, or AMP-PNP, as indicated. The results were graphed (n=3, +/- standard error).

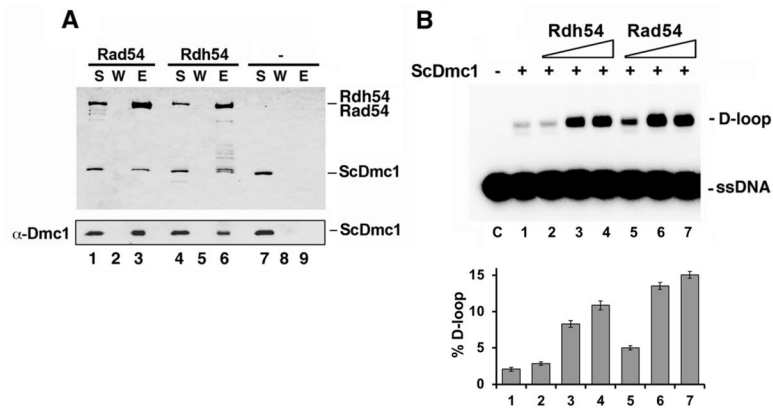


Figure 4. Physical and functional interactions of ScDmc1 with Rad54 and Rdh54
A. ScDmc1 was incubated with S-tagged Rad54 or Rdh54 and protein complexes were captured on S-protein resin, which was washed and treated with SDS to elute bound proteins. The supernatant (S) that contained unbound proteins, wash (W), and SDS eluate (E) were analyzed by SDS-PAGE and Coomassie blue staining (top panel) or immunoblotted with anti-hDMC1 antibody (bottom panel). **B.** Comparison of ScDmc1 D-loop activity in the presence of Rad54 and Rdh54. The results were graphed (n=3, +/- standard error).

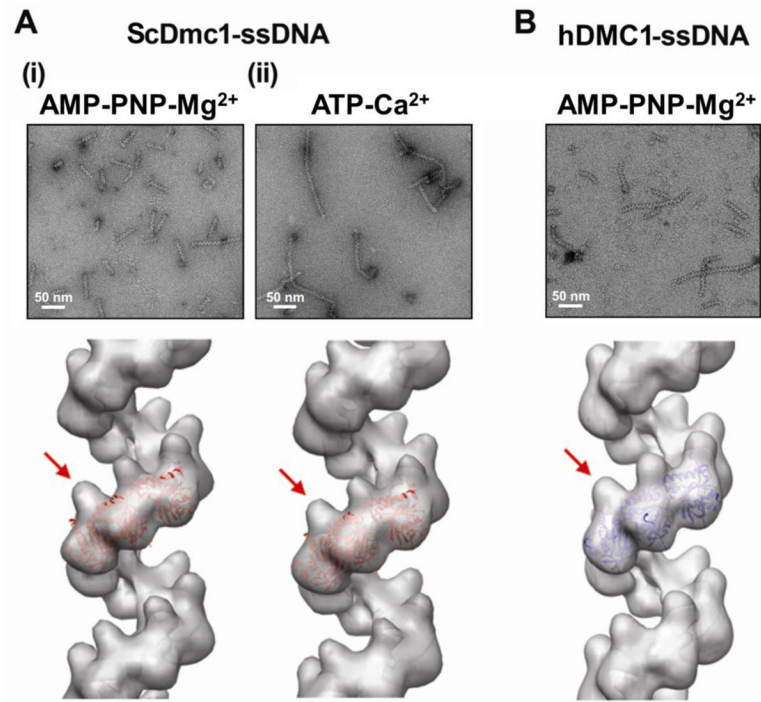


Figure 5. EM and 3D reconstructions of ScDmc1 and hDMC1 filaments on ssDNA
 The top panels show negative stained presynaptic filaments of ScDmc1 (**A**) and hDMC1 (**B**) assembled with AMP-PNP-Mg²⁺ (**A(i)**, **B**) or ATP-Ca²⁺ (**A(ii)**). The 3D reconstructions of the presynaptic filaments are shown in the bottom panels. Arrow indicates the N-terminal domains (NTD) of each protein. The hDMC1 (Pro83-Glu340) crystal structure (PDB: 1V5W) was docked in the 3D maps.